Design of an optofluidic sensor for rapid detection of hemolysis

Edikan Archibong,[1,2] Justin Stewart,[1] Hao Wang,[1] Anna Pyayt[1*]
[1]Innovative Biomedical Instruments and Systems (IBIS) Laboratory, Department of Chemical & Biomedical Engineering, University of South Florida, 4202 E. Fowler Avenue, Tampa, FL 33260, USA
[2]Department of Medicine, University of North Carolina at Chapel Hill, NC 27599, USA

ABSTRACT

Blood tests are a vital source of information for disease diagnosis and monitoring. Blood sample contamination due to hemolysis (the rupturing of red blood cells) is a significant problem that can result in incorrect diagnoses, delayed treatment, and inappropriate prescriptions. Therefore, a simple, rapid test is needed to detect the occurrence of hemolysis. Here we propose a new miniature spectroscopic device, integrated onto an optical fiber platform, which can quickly and reliably determine the amount of free hemoglobin in a small droplet of blood plasma. Optimal design parameters for the device were calculated theoretically, and then the device was fabricated and tested. Experimental tests demonstrated that the device could quickly measure free plasma hemoglobin over a wide range of concentration (0–500 mg/dL) and with a low detection limit (<4 mg/dL), sufficient to detect both low- and high-grade hemolysis in a droplet of blood plasma. This device can, therefore, be useful for rapid quality control in blood-testing laboratories, hospitals, and dialysis settings.

Keywords: *blood testing, sample quality control, hemolysis*

***Corresponding author e-mail:** pyayt@usf.edu

1. Introduction

Every day millions of blood samples are collected in hospitals and clinics for medical analysis [1,2], but a significant portion of these samples are compromised due to hemolysis (the rupturing of red blood cells, which releases hemoglobin and other intracellular components into the blood plasma). Up to 31% of samples drawn in emergency rooms and 10% of samples drawn in blood banks and blood-testing facilities are thus compromised [3,4]. Significant effort has therefore been devoted to reducing the rate of hemolysis associated with collection techniques (e.g., through the use of appropriate needles), but no significant improvement has been demonstrated [4,5]. Post-collection hemolysis may also occur due to a variety of causes such as improper sample handling, transportation, or storage [4,6]. Given the difficulty of eliminating the occurrence of hemolysis, detecting the presence of hemolytic contaminants in blood plasma is critical.

Annually, millions of dollars are wasted, and many diagnoses are delayed due to the contamination of blood samples by hemolysis. Some tests produce erroneous results, and, overall, hemolysis is the leading cause of pre-analytical errors [5,7]. The presence of hemoglobin in plasma results in incorrect measurements of important blood components as lactate dehydrogenase (LD), aspartate aminotransferase (AST), bilirubin, cholesterol, and glucose. Currently, visual detection of hemolysis is the standard-of-care criterion for laboratory rejection of samples for analysis. However, the quality of blood-test results can be compromised even when the level of free plasma hemoglobin is visually undetectable (less than 50 mg/dL) [8].

At present, there is no reliable way to detect hemolysis without first separating the blood plasma from the whole blood sample. The traditional detection method is a visual assessment of the level of "redness" of the separated plasma. This approach, however, results in a high percentage of human error and miscategorization. Alternatively, there are several technologies to measure hemoglobin in free plasma, such as enzyme-linked immunosorbent assay (ELISA) and spectrophotometry [9-13]. These methods, however, are time-consuming and expensive, and they do not work well for rapid assessments of sample quality. Additionally, these technologies require large volumes of blood (milliliters). Common analytical systems used for these analyses are the Roche Modular System, Integra 400 Plus, Siemens Dimension RxL, ADVIA 2400 and ADVIA 1800, Olympus AU 680, and Coulter DXC 800. With this approach, samples are collected from patients, processed, and then shipped to laboratory facilities for testing — a process that can take up to 2 days before samples are received and evaluated [14].

Here we propose a new miniature device that uses absorption spectroscopy to determine the level of hemolysis by measuring hemoglobin concentration in a drop of plasma. The method is reagent-free, and quantitative results are available immediately. Such a device, miniature and portable, could be beneficial in numerous applications — for example, for quality control of blood samples received at blood-testing facilities or of blood products to be delivered in hospital transfusions. (Hemolyzed plasma can be dangerous to patients.) Such devices could also be the basis of integrated systems to detect, in real time, hemolysis by dialysis machines. Such machines may mechanically damage patients' red blood cells, but this damage is currently difficult to detect.

2. Device design and packaging

Traditionally, hemolysis cannot be visually assessed in whole blood samples because of interference from unlysed red blood cells (RBCs). RBCs must first be separated so that the plasma alone can be analyzed for the presence and concentration of hemoglobin. This analysis can be achieved by centrifugation followed by measurement of the absorption spectrum of the separated plasma. Alternatively, measurements can be conducted on the thin layer of plasma that quickly forms in whole blood samples due to blood cell sedimentation. For the small volumes of plasma required for the approach proposed in this work, the latter approach is adequate.

Fig. 1a shows the conceptual design of an optical fiber platform to be used to make spectrophotometric measurements on a small volume of plasma (microliters). An optical fiber inside of a capillary tube is fitted within a sample chamber made of polydimethylsiloxane (PDMS). Plasma enters the sample holder through the pores of a reflective micro-membrane at the base of the chamber. This design, which was optimized through theoretical analysis (as described in section 3), allows for the analysis of a very small volume of plasma.

Fig. 1b shows the assembled prototype, with the cleaved optical fiber pointing toward the reflective surface. The optical fiber is positioned within the capillary tube, which is integrated with the PDMS sample holder. The use of the capillary tube allows the fiber to be moved up and down without loss of orientation so that the effects of different distances (ℓ) between the fiber tip and the reflector membrane can be experimentally determined. The following optical components were used for the prototype: optical fiber FT200EMT (0.39 NA, 200 μm core), a Ventus 532 green laser from Laser Quantum, and a PM320E dual-channel optical power and energy meter from ThorLabs.

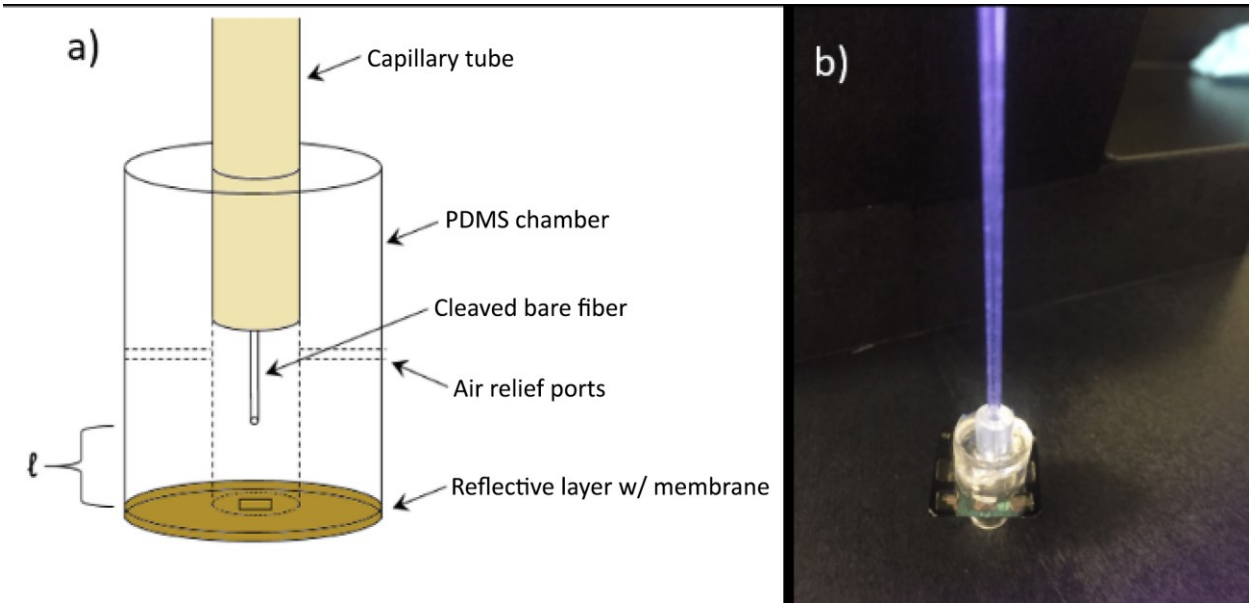

Fig. 1. Spectroscopic probe to measure hemoglobin in a small sample of blood plasma. (a) Conceptual design. An optical fiber is inserted into a PDMS chamber that contains the plasma sample. The distance between the reflective surface and fiber tip is indicated as ℓ (~1 mm). (b) Photograph of fully assembled prototype probe.

The bottom of the PDMS chamber (Fig. 1a) consists of a custom-fabricated thin (~1 μm) reflective porous membrane of silicon nitride. This membrane is fabricated using a conventional photolithographic process followed by gold deposition [15-17]. Specifically, silicon nitride was deposited on both sides of a silicon wafer, and a positive

resist was used for design patterning. Pores (1–3 μm in diameter) were then etched, using photolithography, across the entire membrane in a square array. After this photolithography and nitride etching, wet-etching across the whole silicon substrate was performed, and a 200 nm thickness of gold was deposited on the membrane to act as a reflective layer. Finally, the supporting wafer was attached to the PDMS tube with epoxy to ensure a watertight seal.

For each analysis, a 50 μl drop of plasma (analytical sample) is placed on the surface of the membrane. Due to capillary action, this droplet is drawn into the device. The spectroscopic analysis is then performed to measure the concentration of free hemoglobin within the plasma sample. Light from the single optical fiber tip, which is immersed in the plasma sample, passes through the fluid to eventually reach the gold-coated reflective membrane. The reflected light is then coupled back to the optical fiber and sent to a power meter for measurement. For multiple measurements conducted using the same device, the device can be cleaned by quick immersion into acetone followed by a brief wash in water and ethanol. One-time use is also feasible because the production of multiple devices (100s to 1000s of devices) on a single silicon wafer allows for low-cost mass fabrication (less than USD 1 per device).

3. Optimization of optical design parameters

The concentration of hemoglobin in blood plasma is determined by measuring light transmission through the sample droplet. The Beer-Lambert law relates light transmission to the concentration of optically absorptive compounds in a sample:

$$T_\ell = \exp(-2\alpha\ell C) \qquad (1)$$

where α is the wavelength-dependent molar absorptivity of hemoglobin (L/mol·cm), ℓ is the distance between the tip of the optical fiber and the reflective membrane (cm) (Fig. 1a), C is the concentration of hemoglobin in the plasma (mol/L), and T_ℓ is the resulting fraction of light transmitted through the sample of thickness ℓ, in which the fiber tip is immersed.

Hemoglobin occurs naturally in two forms (oxygenated and deoxygenated), which have different molar absorptivities. At a few wavelengths (isosbestic points), α is the same for both forms. The advantage of performing measurements at isobestic points is that a single wavelength can be used to conveniently determine the total concentration of hemoglobin (i.e., both forms combined). For hemoglobin, four isosbestic points occur within the wavelength range of 500–600 nm, at approximately 530, 545, 570, and 584 nm, with α values of 0.0138, 0.0188, 0.0167, and 0.0127 L/mol·cm, respectively [18]. For this work, a wavelength of 545 nm was selected because of the high corresponding absorptivity.

Having chosen the wavelength (thus fixing the value of α in Eq. 1), there remain three unknown variables. Hemoglobin concentration C is the variable we wish to determine, and transmission T_ℓ is the variable we can directly measure. The distance ℓ can then be chosen such that the sensor operates optimally for the detection of hemolysis products.

Fabrication of a device with an appropriate distance between the gold-coated membrane and the optical fiber is important for accurate measurement of the hemoglobin concentration in a plasma sample [15]. Fig. 2 shows the theoretical influence of the distance ℓ (Fig. 1a) on the transfer function that relates normalized light transmission to total hemoglobin concentration. (These functions were generated using Eq 1.) With this information, the optimal fiber spacing distance can be chosen based on the range of analytical conditions. For example, if expected hemoglobin concentrations range up to only 100 mg/dL (moderately hemolyzed), then a larger fiber spacing distance (4.0 mm) would be chosen to achieve the best resolution. The thicker layer of sample plasma would allow for greater optical absorption and the extraction of most information at low hemoglobin concentrations. For higher concentrations, smaller distances would be chosen. The discussion that follows describes how we quantitatively identified the optimal spacing for our target range of 0 to 500 mg/dL.

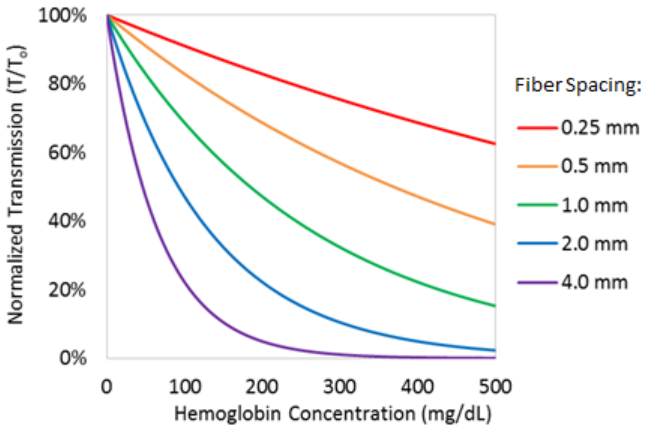

Fig. 2. Theoretical transfer functions relating normalized light transmission to hemoglobin concentrations for different spacing distances ℓ between the fiber tip and the reflective membrane at wavelength 545 nm.

For a sensor that displays exponential decay as its operating curve, we consider performance to be optimal when there exists a strong negative decay over the concentration range of interest. This characteristic allows for distinct and well-defined changes in transmission, as well as higher sensitivity in resolving concentration values. However, the performance curve must not display too steep an exponential decay, as the sensor would then lose sensitivity in resolving concentrations at the extremities of the range of interest.

To characterize sensor behavior over a range of hemoglobin concentrations, two operation parameters were created through manipulations of statistical curve regression analysis and least squares error: (1) the fraction of maximum decay ψ and (2) the degree of curvature φ. We used these parameters to refine the conceptual design of the spectroscopic probe (Fig. 1a) before fabrication of the prototype (Fig. 1b).

The fraction of maximum decay ψ is a measure of how much the signal 'decays' over the concentration range of interest (C_a to C_b). A value of zero indicates a curve with no decay, while a value of one implies that maximum decay has been reached over the range of interest (i.e., transmission at C_b is 0%). Derivation and simplification of this parameter are shown in Eq. 2:

$$\psi = \left(\frac{T_\ell(C_b) - T_\ell(C_a)}{C_b - C_a}\right)\left(\frac{C_b - C_a}{T_\infty(C_b) - T_\infty(C_a)}\right) = 1 - \frac{T_\ell(C_b)}{100\%} \qquad (2)$$

Here, transmission T_ℓ is a function of concentrations C_a and C_b, and the subscript ℓ signifies that the separation between the fiber and the membrane is fixed at length ℓ. As such, T_∞ is the transmission that corresponds to a fixed separation for which the tip of the optical fiber and the reflective membrane are infinitely far apart.

The other parameter, the degree of curvature φ, measures the extent to which the exponential sensor deviates from a linear operation behavior. A degree of curvature near one indicates that the curve is behaving approximately linearly. As this value decreases, the operation curve deviates from a linear fit. This parameter was derived through modification of the least squares correlation coefficient, to describe the squared error between the exponential operation curve T_ℓ and a hypothetical performance curve for a linear sensor θ_l. Expressions for φ and θ_ℓ are given in Eqs. 3 and 4:

$$\phi = 1 - \frac{\int_{C_a}^{C_b}(\theta_\ell - T_\ell)^2 dC}{\int_{C_a}^{C_b}(\theta_\infty - T_\infty)^2 dC} = 1 - \frac{\int_{C_a}^{C_b}(\theta_\ell - T_\ell)^2 dC}{\int_{C_a}^{C_b}(\theta_\infty)^2 dC} \qquad (3)$$

$$\theta_\ell = \left(\frac{T_\ell(C_b) - T_\ell(C_a)}{C_b - C_a}\right) \cdot C + 100\% \qquad (4)$$

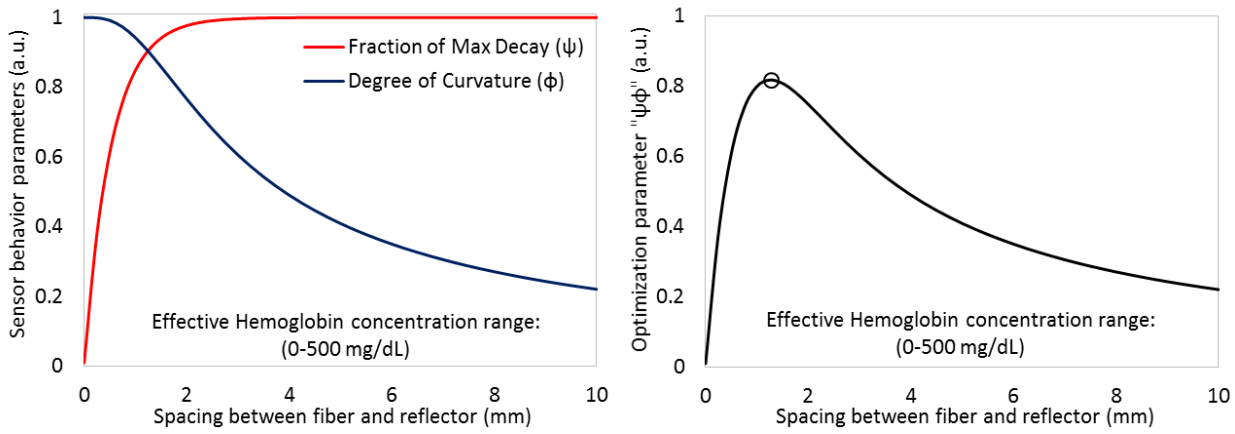

Fig. 3. Sensor parameter optimization for optical detection of plasma hemoglobin over the concentration range of 0–500 mg/dL. (a) Parameters describing sensor behavior (φ and ψ) as a function of chamber length ℓ. (b) The product of these two parameters as a function of chamber length ℓ. The maximum value (marked by the black circle) indicates the distance required for optimum optical performance. a.u. = arbitrary units

Solving Eqs. 1 through 4 for the hemoglobin concentration range of 0–500 mg/dL and iterating over various distances ℓ, the two behavior parameters can be calculated (Fig. 3a). When the distance is near 0 mm (i.e., fiber and membrane are nearly touching), the sensor behaves nearly linearly (i.e., φ is nearly 1); however, the rate of decay is significantly low. Conversely, as the separation length increases, the decay rapidly reaches its maximum value; however, the sensor operates exponentially. By multiplying the two parameters (φψ), the optimum behavior can be determined by locating the relative maximum value, which in turn reveals the optimal distance required to achieve this desired behavior. Fig. 3b shows the results of this multiplication, with a maximum product value at $\ell_m \cong 1.27$ mm. We, therefore, chose this distance for the final design of the spacing between the optical fiber and the membrane.

Fig. 4 shows the theoretical transfer function obtained by solving the Beer-Lambert law (Eq. 1) for optimal distance $\ell = 1.27$ for the hemolysis sensor. With optimum chamber length, this operating curve for the sensor can be achieved. The curve in Fig. 4 indicates that the decline in transmission between a sample of pure plasma (0 mg/dL of hemoglobin) and a slightly hemolyzed sample (30 mg/dL of hemoglobin) is approximately 13%.

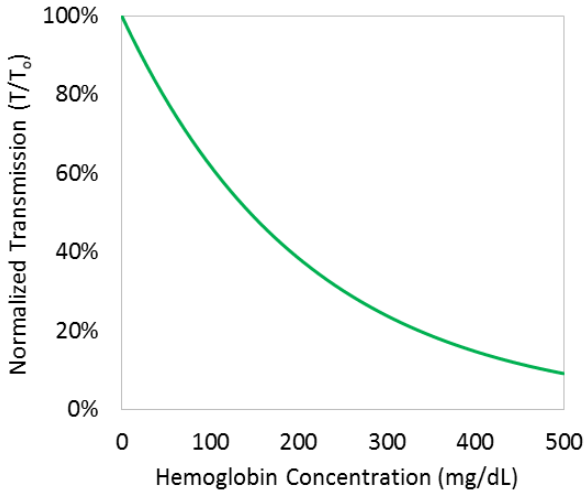

Fig. 4. Theoretical performance curve for the optimum sensor configuration where $\ell = 1.27$ mm, over a hemoglobin concentration of 0–500 mg/dL.

The calculations described in section 3 do not take into consideration diffraction of the light shining out of the optical fiber, which results in decreased back coupling. As a result, the optimal spacing distance would be smaller than the theoretical value of 1.27 mm. Also, light propagates through the plasma layer two times because of reflection from the gold surface. Therefore the gap should be half the value calculated for the single pass (i.e., optimal ℓ = 0.64 mm).

To experimentally determine the optimal spacing distance, the fiber holder was inserted into a capillary tube, which was then connected to an XYZ-stage and adjusted to a distance of about 1 mm from the gold surface. The system was optically aligned by adjusting the XYZ-stage and observing the reflected power when the sample chamber was filled with either air or water. The recorded Fabry-Perot resonance formed between the cleaved fiber and the gold surface was used to determine the precise distance and to adjust it to the needed (optimum) value [15]. Fig. 5 shows results for theoretical and experimental determinations of the percentage of light lost due to diffraction under different conditions (i.e., for different fiber diameters and different chamber contents). For the fiber–reflector gap we are interested in (i.e., between 0 and 1 mm), the optical fiber of 200 µm core diameter loses the least amount of light (Fig. 5a). Therefore, all subsequent measurements were conducted with a fiber of this diameter. For the determination of light losses in air and water (Fig. 5b), the theoretical results and the experimental data were in good agreement. It is worth noting that for mass production the precise alignment using XYZ-stage is not required, since, according to the theoretical optimization distance fluctuation within ±100µm would not significantly degrade the sensor's performance.

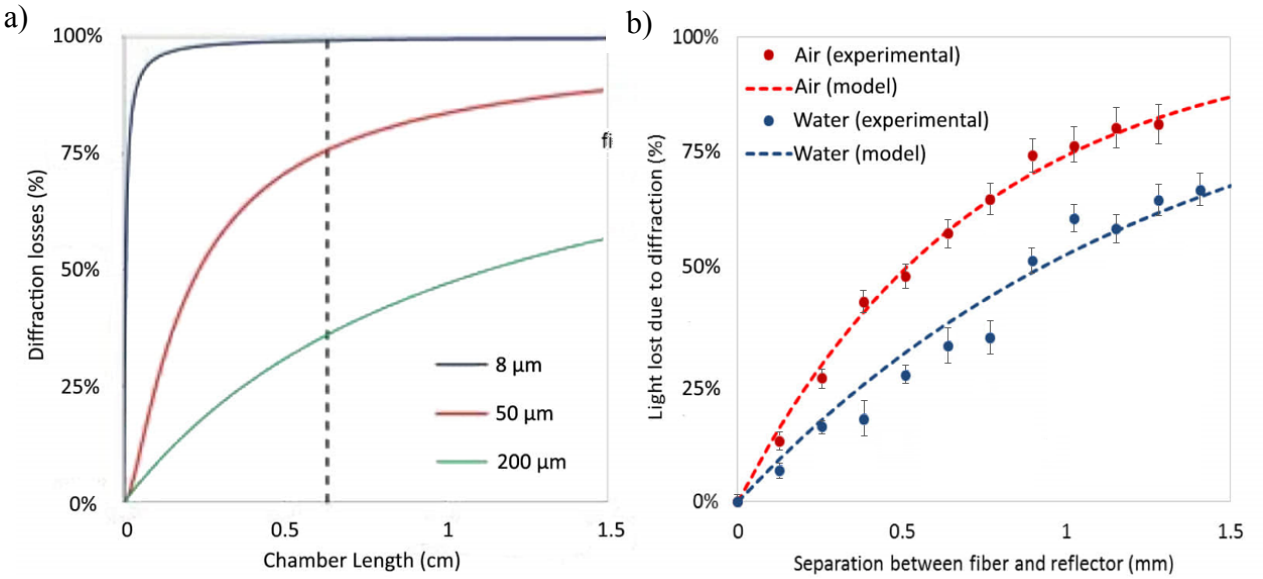

Fig. 5. Experimental and theoretical model. (a) Left Panel: Modeled percentage of light loss due to diffraction as a function of chamber length for optical fibers of different core diameters. (b) Right panel: Percentage of light loss due to diffraction as a function of chamber length, when the chamber was filled with either air (red) or water (blue). The dots represent the experimental data, while the dashed curves indicate modeled fits.

4. Experimental detection of hemoglobin

Serial solutions of hemoglobin in blood plasma were formulated over the range of 0–500 mg/dL with 50 mg/dL intervals, using blood plasma and hemoglobin from bovine blood lyophilized powder. Two-way transmission measurements of each sample (i.e., at each concentration) were taken and signal-averaged over 5-minute intervals. All measurements were normalized relative to initial laser power. The results (Fig. 6) show an exponential decay of reflected light intensity, Power, with increasing concentrations of hemoglobin (due to increased light absorption) as well as weak periodic fluctuations of intensity due to the change of refractive index in the Fabry-Perot resonator [19]. These results indicate optimized sensor behavior. At low hemoglobin concentrations, differences as small as 4 mg/dL can be readily measured. Specifically, Fig. 6 shows that the entire range of physiologically relevant hemoglobin values can be measured with this new sensor, from virtually hemoglobin-free to grossly hemolyzed (500 mg/dL). The detection limit is 4 mg/dL.

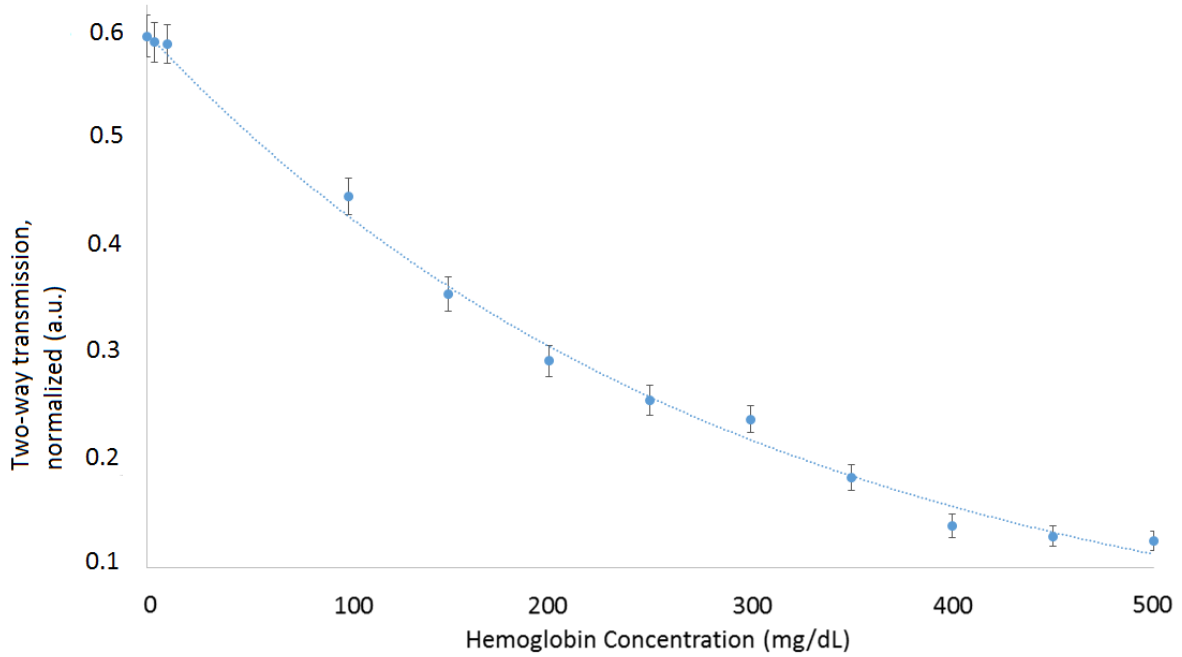

Fig. 6. A two-way transmission as a function of hemoglobin concentration. Each data point shows the average of reflected power measurements collected each over a period of 5 minutes at intervals. The dotted line shows. a.u. = arbitrary units

5. Conclusion

The ability to rapidly detect hemolysis, using only microliters of blood plasma, has many critical applications related to quality and safety control of various types of blood tests. In this work, we theoretically optimized, physically fabricated, and experimentally tested a miniature instrument to rapidly screen for hemolysis in plasma samples over a broad range of hemoglobin concentrations (0–500 mg/dL). This sensor has a very low detection limit, just 4 mg/dL (as compared to 50 mg/dL for conventional detection methods based on human vision). This sensing platform integrates optical fiber–based spectroscopy with microfluidics for not only reliable detection of hemolysis but also quantitatively accurate measurements of free plasma (total) hemoglobin concentrations. The spectrophotometric results are available immediately. Integration of such instruments into routine blood testing would improve the reliability of routine blood tests, decrease testing errors, and overall significantly benefit healthcare outcomes.

6. Acknowledgments

The authors thank the University of South Florida Nanotechnology Research and Education Center (NREC) for providing a platform for all fabrication work and Dr. Tonya Clayton for her editorial assistance.

FUNDING: The laboratory of A. Pyayt is supported by the National Science Foundation [grant number 1701081]. E. Archibong was supported by the Alfred P. Sloan Foundation Minority Ph.D. Program and the Florida Education Fund's Mcknight Fellowship Program Dissertation Awards.

References

1. Zhdanov, A., Keefe, J., Franco-Waite, L., Konnaiyan, K. R., & Pyayt, A. (2018). Mobile phone-based ELISA (MELISA). Biosensors and Bioelectronics, 103, 138-142.

2. Archibong, E., Konnaiyan, K. R., Kaplan, H., & Pyayt, A. (2017). A mobile phone-based approach to detection of hemolysis. Biosensors and Bioelectronics, 88, 204-209.

3. Giuseppe Lippi, G.C., Emmanuel J. Favaloro, Mario Plebani, *Hemolysis, An Unresolved Dispute in Laboratory Medicine*, in *In Vitro and In Vivo Hemolysis*. 2012.

4. Stauss, M., et al., *Hemolysis of coagulation specimens: a comparative study of intravenous draw methods.* Journal of Emergency Nursing, 2012. **38**(1): p. 15-21.
5. Lippi, G., et al., *Special issue: Quality in laboratory diagnostics: from theory to practice.* Biochemia Medica, 2010. **20**(2): p. 126-30.
6. McGrath, J.K., P. Rankin, and M. Schendel, *Let the data speak: decreasing hemolysis rates through education, practice, and disclosure.* Journal of Emergency Nursing, 2012. **38**(3): p. 239-244.
7. Makroo, R.N., et al., *Evaluation of Red Cell Hemolysis in Packed Red Cells During Processing and Storage.* Apollo Medicine, 2010. **7**(1): p. 35-38.
8. Koseoglu, M., et al., *Effects of hemolysis interference on routine biochemistry parameters.* Biochemia Medica, 2011. **21**(1): p. 79-85.
9. Schaer, D.J. et al., *Hemolysis and free hemoglobin revisited: exploring hemoglobin and hemin scavengers as a novel class of therapeutic proteins.* Blood, 2013. **121**(8): p. 1276-1284.
10. Adamzik, M., et al., *Free hemoglobin concentration in severe sepsis: methods of measurement and prediction of outcome.* Critical Care, 2012. **16**(4): p. R125.
11. Harboe, M., *A Method for Determination of Hemoglobin in Plasma by Near-Ultraviolet Spectrophotometry.* Scandinavian Journal of Clinical & Laboratory Investigation, 1959. **11**(1): p. 66-70.
12. Fairbanks, V., S. Ziesmer, and P. O'Brien, *Methods for measuring plasma hemoglobin in micromolar concentration compared.* Clinical chemistry, 1992. **38**(1): p. 132-140.
13. Noe, D.A., V. Weedn, and W.R. Bell, *Direct spectrophotometry of serum hemoglobin: an Allen correction compared with a three-wavelength polychromatic analysis.* Clinical chemistry, 1984. **30**(5): p. 627-630.
14. Lippi, G., Salvagno, G.L., Blanckaert, N., Giavarina, D., Green, S., Kitchen, S., Palicka, V., Vassault, A.J. and Plebani, M., *Multicenter evaluation of the hemolysis index in automated clinical chemistry systems*. Clinical chemistry and laboratory medicine, 2009. **47**(8): p.934-939.
15. Archibong, E., Stewart, J., and Pyayt, A., *Optofluidic spectroscopy integrated on optical fiber platform.* Sensing and Bio-Sensing Research, 2015. **3**(0): p. 1-6.
16. Cheemalapati, S., Ladanov, M., Winskas, J., & Pyayt, A. (2014). Optimization of dry etching parameters for fabrication of polysilicon waveguides with smooth sidewall using a capacitively coupled plasma reactor. Applied Optics, 53(25), 5745-5749.

17. Archibong, E., Tuazon, H., Wang, H., Winskas, J., & Pyayt, A. L. (2016). Modular Microfluidic Filters Based on Transparent Membranes. Journal of Electronic Packaging, 138(4), 041002.

18. Prahl, S., *Tabulated Molar Extinction Coefficient for Hemoglobin in Water.*

19. Zhu, J. M., Y. Shi, X. Q. Zhu, Y. Yang, F. H. Jiang, C. J. Sun, W. H. Zhao, and X. T. Han., *Optofluidic marine phosphate detection with enhanced absorption using a Fabry–Pérot resonator*. Lab on a Chip, 2017. **17** (23): p. 4025-4030.